

# The initial energy density of gluons produced in very high energy nuclear collisions

Alex Krasnitz

*UCEH, Universidade do Algarve, Campus de Gambelas, P-8000 Faro, Portugal.*

Raju Venugopalan

*Physics Department, Brookhaven National Laboratory, Upton, NY 11973, USA.*

February 7, 2008

## Abstract

In very high energy nuclear collisions, the initial energy of produced gluons per unit area per unit rapidity,  $dE/L^2/d\eta$ , is equal to  $f(g^2\mu L)(g^2\mu)^3/g^2$ , where  $\mu^2$  is proportional to the gluon density per unit area of the colliding nuclei. For an SU(2) gauge theory, we perform a non-perturbative numerical computation of the function  $f(g^2\mu L)$ . It decreases rapidly for small  $g^2\mu L$  but varies only by  $\sim 25\%$ , from  $0.208 \pm 0.004$  to  $0.257 \pm 0.005$ , for a wide range 35.36–296.98 in  $g^2\mu L$ , including the range relevant for collisions at RHIC and LHC. Extrapolating to SU(3), we estimate the initial energy per unit rapidity for  $Au$ – $Au$  collisions in the central region at RHIC and LHC.

By the end of 1999, the Relativistic Heavy Ion collider (RHIC) at BNL will begin colliding beams of  $Au$ –ions at  $\sqrt{s} = 200$  GeV/nucleon. Some years later, the Large Hadron collider (LHC) at CERN will collide heavy ions at  $\sqrt{s} \approx 5.5$  TeV/nucleon. The objective of these experiments is to understand the properties of very hot and dense partonic matter in QCD. It is of considerable interest to determine whether this hot and dense matter equilibrates to briefly form a plasma of quarks and gluons (QGP) [1].

The dynamical evolution of such a system clearly depends on the initial conditions, namely, the parton distributions in the nuclei prior to the collision. For partons with transverse momenta  $p_t \gg \Lambda_{QCD}$ , cross-sections in the standard perturbative QCD approach may be computed by convolving the parton distributions of the two nuclei with the elementary parton–parton scattering cross sections. At the high energies of the RHIC (LHC) collider, hundreds (thousands) of mini-jets with  $p_t$ 's of the order of several GeV may be formed [2]. Final state interactions of these mini-jets are often described in multiple scattering (see Ref. [3] and references therein) or in classical cascade approaches (see

Ref. [4] and references therein). Estimates for the initial energy density in a self screened parton cascade approach can be found in Ref. [5].

At central rapidities, where  $x \ll 1$ , and  $p_t \gg \Lambda_{QCD}$  with  $x$  defined to be  $p_t/\sqrt{s}$ , parton distributions grow rapidly, and may even saturate for large nuclei for  $x$ 's in the range  $10^{-2}$  to  $10^{-3}$  relevant for nuclear collisions at RHIC and LHC respectively [6, 7]. Coherence effects are important here, and are only included heuristically in the above mentioned perturbative approaches.

In this letter, we will describe results from a classical effective field theory (EFT) approach which includes coherent effects in the small  $x$  parton distributions of large nuclei [8]. If the parton density in the colliding nuclei is large at small  $x$ , classical methods are applicable. It has been shown recently that a renormalization group improved generalization of this effective action reproduces several key results in small  $x$  QCD: the leading  $\alpha_S \log(1/x)$  BFKL equation, the double log GLR equation and its extensions, and the small  $x$  DGLAP equation for quark distributions [9, 10]. It has also been argued, from other considerations, that the main results of this model should be general results in small  $x$  QCD [6].

The EFT contains one dimensionful parameter  $\mu^2$ , which is the variance of a Gaussian weight over the color charges  $\rho^\pm$  of partons, of each nucleus, at rapidities higher than the rapidity of interest. For central impact parameters, it is determined to be [11]

$$\mu^2 = \frac{A^{1/3}}{\pi r_0^2} \int_{x_0}^1 dx \left( \frac{1}{2N_c} q(x, Q^2) + \frac{N_c}{N_c^2 - 1} g(x, Q^2) \right), \quad (1)$$

where  $xq(x, Q^2)$  and  $xg(x, Q^2)$  stand for the *nucleon* quark and gluon structure functions at the resolution scale  $Q$  of the physical process of interest. Also, one has  $x_0 = Q/\sqrt{s}$ ,  $r_0 = 1.12$  fm, and  $N_c$  is the number of colors. From the HERA data for  $q$  &  $g$ , one obtains  $\mu \leq 1$  GeV for LHC energies and  $\mu \leq 0.5$  GeV at RHIC [11]. The classical gauge fields, and hence the classical parton distributions, can be determined analytically [9, 12]. On this basis, it has been argued recently that the typical transverse momenta scale  $Q_s$  in this model is further in the weak coupling regime, with  $Q_s \sim 1$  GeV for RHIC and  $Q_s \sim 2-3$  GeV at LHC [29].

Kovner, McLerran and Weigert [13] applied the effective action approach to nuclear collisions. (For an interesting alternative approach, see Ref. [14].) Assuming boost invariance, and matching the equations of motion in the forward and backward light cone, they obtained the following initial conditions for the gauge fields in the  $A^\tau = 0$  gauge:  $A_\perp^i|_{\tau=0} = A_1^i + A_2^i$ , and  $A^\pm|_{\tau=0} = \pm \frac{ig}{2} x^\pm [A_1^i, A_2^i]$ . Here  $A_{1,2}^i(\rho^\pm)$  ( $i = 1, 2$ ) are the pure gauge transverse gauge fields corresponding to small  $x$  modes of incoming nuclei (with light cone sources  $\rho^\pm \delta(x^\mp)$ ) in the  $\theta(\pm x^-)\theta(\mp x^+)$  regions respectively of the light cone.

The sum of two pure gauges in QCD is not a pure gauge—the initial conditions therefore give rise to classical gluon radiation in the forward light cone. For  $p_t \gg \alpha_S \mu$ , the Yang–Mills equations may be solved perturbatively to quadratic order in  $\alpha_S \mu/p_t$ . After averaging over the Gaussian random sources of color charge  $\rho^\pm$  on the light cone,

the perturbative energy and number distributions of physical gluons were computed by several authors [13, 11, 15, 16, 17]. In the small  $x$  limit, it was shown that the classical Yang–Mills result agreed with the quantum Bremsstrahlung result of Gunion and Bertsch [18].

In Ref. [19], we suggested a lattice discretization of the classical EFT, suitable for a non-perturbative numerical solution. Assuming boost invariance, we showed that in  $A^\tau = 0$  gauge, the real time evolution of the small  $x$  gauge fields  $A_\perp(x_t, \tau)$ ,  $A^\eta(x_t, \tau)$  is described by the Kogut–Susskind Hamiltonian in 2+1-dimensions coupled to an adjoint scalar field. The lattice equations of motion for the fields are then determined straightforwardly by computing the Poisson brackets. The initial conditions for the evolution are provided by the lattice analogue of the continuum relations discussed earlier in the text. We impose periodic boundary conditions on an  $N \times N$  transverse lattice, where  $N$  denotes the number of sites. The physical linear size of the system is  $L = aN$ , where  $a$  is the lattice spacing. It was shown in Ref. [20] that numerical computations on a transverse lattice agreed with lattice perturbation theory at large transverse momentum. For details of the numerical procedure, and other details, we refer the reader to Ref. [20].

In this letter, we will focus on computing the energy density  $\varepsilon$  as a function of the proper time  $\tau$ . This computation on the lattice is straightforward. Our main result is contained in Eq. 2. To obtain this result, we compute the Hamiltonian density on the lattice for each  $\rho^\pm$ , and then take the Gaussian average (with the weight  $\mu^2$ ) over between 40  $\rho$  trajectories for the larger lattices and 160  $\rho$  trajectories for the smallest ones.

In our numerical simulations, all the relevant physical information is compressed in  $g^2\mu$  and  $L$ , and in their dimensionless product  $g^2\mu L$  [21]. The strong coupling constant  $g$  depends on the hard scale of interest; from Eq. 1, we see that  $\mu$  depends on the nuclear size, the center of mass energy, and the hard scale of interest;  $L^2$  is the transverse area of the nucleus [30]. Assuming  $g = 2$  (or  $\alpha_S = 1/\pi$ ),  $\mu = 0.5$  GeV (1.0 GeV) for RHIC (LHC), and  $L = 11.6$  fm for  $Au$ -nuclei, we find  $g^2\mu L \approx 120$  for RHIC and  $\approx 240$  for LHC. (The latter number would be smaller for a smaller value of  $g$  at the typical LHC momentum scale.) As will be discussed later, these values of  $g^2\mu L$  correspond to a region in which one expects large non-perturbative contributions from a sum to all orders in  $\sim 6\alpha_S\mu/p_t$ , even if  $\alpha_S \ll 1$ . We should mention here that deviations from lattice perturbation theory, as a function of increasing  $g^2\mu L$ , were observed in our earlier work [20].

We shall now discuss results from our numerical simulations. In Fig. 1, we plot  $\varepsilon\tau/(g^2\mu)^3$ , as a function of  $g^2\mu\tau$ , in dimensionless units, for the smallest, largest, and an intermediate value in the range of  $g^2\mu L$ 's studied. The quantity  $\varepsilon\tau$  has the physical interpretation of the energy density of produced gluons  $dE/L^2/d\eta$  only at late times—when  $\tau \sim t$ . Though  $\varepsilon\tau$  goes to a constant in all three cases, the approach to the asymptotic value is different. For the smallest  $g^2\mu L$ ,  $\varepsilon\tau$  increases continuously before saturating at late times. For larger values of  $g^2\mu L$ ,  $\varepsilon\tau$  increases rapidly, develops a transient peak at  $\tau \sim 1/g^2\mu$ , and decays exponentially there onwards, satisfying the relation  $\alpha + \beta e^{-\gamma\tau}$ , to a constant value  $\alpha$  (equal to the lattice  $dE/L^2/d\eta$ !). The lines

shown in the figure are from an exponential fit including all the points past the peak. This behavior is satisfied for all  $g^2\mu L \geq 8.84$ , independently of  $N$ .

Given the excellent exponential fit, one can interpret the decay time  $\tau_D = 1/\gamma/g^2\mu$  as the appropriate scale controlling the formation of gluons with a physically well defined energy. In other words,  $\tau_D$  is the “formation time” in the sense used by Bjorken [22, 31]. In Table 1, we tabulate  $\gamma$  versus  $g^2\mu L$  for the largest  $N \times N$  lattices [32] for all but the smallest  $g^2\mu L$ . For large  $g^2\mu L$ , the formation time decreases with increasing  $g^2\mu L$ , as we expect it should.

In Fig. 2, we plot the asymptotic values  $\alpha$  of  $\varepsilon\tau/(g^2\mu)^3$  as a function of  $g^2\mu a$  for various values of  $g^2\mu L$ . As shown in the upper part of Fig. 2, for smaller  $g^2\mu L$ , one can go very close to the continuum limit with excellent statistics (over 160 independent  $\rho$  trajectories for the two smallest values of  $g^2\mu L$ ). In the lower part of Fig. 2, all the data give straight line fits with good  $\chi$ -squared values. We use these fits to extrapolate the value of  $\alpha$  in the continuum limit. We note that the largest value of  $g^2\mu L$  with the smallest  $g^2\mu a$  equal to 0.247, is relatively much further away from the continuum limit than the points in the upper part of the figure. It is obtained by averaging 40 independent trajectories on a  $1200 \times 1200$  lattice. To lower  $g^2\mu a$  below 0.1, would require going to lattices with  $3000 \times 3000$  sites. This exceeds the CPU memory of our current computational resources. Nevertheless, even for the largest  $g^2\mu L$ , we do get a fine linear fit—though we would warn of a potentially large systematic error in the extrapolated value of  $\varepsilon\tau/(g^2\mu)^3$ .

The physical energy per unit area per unit rapidity of produced gluons can be defined in terms of a function  $f(g^2\mu L)$  as

$$\frac{1}{L^2} \frac{dE}{d\eta} = \frac{1}{g^2} f(g^2\mu L) (g^2\mu)^3. \quad (2)$$

The function  $f$  here is obtained by extrapolating the values in Fig. 2 to the continuum limit. In Fig. 3, we plot the striking behavior of  $f$  with  $g^2\mu L$ . For very small  $g^2\mu L$ 's, it changes very slightly but then changes rapidly by a factor of two from 0.427 to 0.208 when  $g^2\mu L$  is changed from 8.84 to 35.36. From 35.36 to 296.98, nearly an order of magnitude in  $g^2\mu L$ , it changes by  $\sim 25\%$ . The precise values of  $f$  and the errors are tabulated in Table 1.

$g^2\mu L$	5.66	8.84	17.68	35.36	70.7
$f$	$.436 \pm .007$	$.427 \pm .004$	$.323 \pm .004$	$.208 \pm .004$	$.200 \pm .005$
$\gamma$		$.101 \pm .024$	$.232 \pm .046$	$.165 \pm .013$	$.275 \pm .011$
$g^2\mu L$	106.06	148.49	212.13	296.98	
$f$	$.211 \pm .001$	$.232 \pm .001$	$.234 \pm .002$	$.257 \pm .005$	
$\gamma$	$.322 \pm .012$	$.362 \pm .023$	$.375 \pm .038$	$.378 \pm .053$	

Table 1: The function  $f = dE/L^2/d\eta$  and the relaxation rate  $\gamma = 1/\tau_D/g^2\mu$  tabulated as a function of  $g^2\mu L$ .  $\gamma$  has no entry for the smallest  $g^2\mu L$  since there  $\varepsilon\tau/(g^2\mu)^3$  vs  $g^2\mu\tau$  differs qualitatively from the other  $g^2\mu L$  values.

What is responsible for the dramatic change in the behavior of  $f$  as a function of  $g^2\mu L$ ? In  $A^\tau = 0$  gauge, the dynamical evolution of the gauge fields depends entirely on the initial conditions, namely, the parton distributions in the wavefunctions of the incoming nuclei [23]. In the nuclear wavefunction, at small  $x$ , non-perturbative, albeit weak coupling, effects become important for transverse momenta  $Q_s \sim 6\alpha_s\mu$ . The EFT predicts that classical parton distributions which have the characteristic Weizsäcker-Williams  $1/p_t^2$  behaviour for large transverse momenta ( $p_t \gg Q_s$ ) grow only logarithmically for  $p_t \leq Q_s$ . One can therefore think of  $Q_s$  as a saturation scale [29] that tempers the growth of parton distributions at small momenta.

Now on the lattice,  $p_t$  is defined to be  $2\pi n/L$ , where  $n$  labels the momentum mode. The condition that momenta in the wavefunctions of the incoming nuclei have saturated,  $p_t \sim 6\alpha_s\mu$ , translates roughly into the requirement that  $g^2\mu L \geq 13$  for  $n = 1$ . Thus for  $g^2\mu L = 13$ , one is only beginning to sample those modes. Indeed, this is the region in  $g^2\mu L$  in which one sees the rapid change in  $f$ . The rapid decrease in  $f$  is likely because the first non-perturbative corrections are large, and have a negative sign relative to the leading term. Understanding the later slow rise and apparent saturation with  $g^2\mu L$  requires a better understanding of the number and energy distributions with  $p_t$ . This work is in progress and will be reported on separately [24].

Our results are consistent with an estimate by A. H. Mueller [25] for the number of produced gluons per unit area per unit rapidity. He obtains  $dN/L^2/d\eta = c(N_c^2 - 1)Q_s^2/4\pi^2\alpha_s N_c$ , and argues that the number  $c$  is a non-perturbative constant of order unity. If most of the gluons have  $p_t \sim Q_s$ , then  $dE/L^2/d\eta = c'(N_c^2 - 1)Q_s^3/4\pi^2\alpha_s N_c$  which is of the same form as our Eq. 2. In the  $g^2\mu L$  region of interest, our function  $f \approx 0.23$ – $0.26$ . Using the relation between  $Q_s$  and  $g^2\mu$  [29], we obtain  $c' = 4.3$ – $4.9$ . Since one expects a distribution in momenta about  $Q_s$ , it is very likely that  $c'$  is at least a factor of 2 greater than  $c$ —thereby yielding a number of order unity for  $c$  as estimated by Mueller. This coefficient can be determined more precisely when we compute the non-perturbative number and energy distributions.

We will now estimate the initial energy per unit rapidity of produced gluons at RHIC and LHC energies. We do so by extrapolating from our SU(2) results to SU(3) assuming the  $N_c$  dependence to be  $(N_c^2 - 1)/N_c$  as in Mueller's formula. At late times, the energy density is  $\varepsilon = (g^2\mu)^4 f(g^2\mu L) \gamma(g^2\mu L)/g^2$ , where the formation time is  $\tau_D = 1/\gamma(g^2\mu L)/g^2\mu$  as discussed earlier. We find that  $\varepsilon^{RHIC} \approx 66.49$  GeV/fm<sup>3</sup> and  $\varepsilon^{LHC} \approx 1315.56$  GeV/fm<sup>3</sup>. Multiplying these numbers by the initial volumes at the formation time  $\tau_D$ , we obtain the classical Yang-Mills estimate for the initial energies per unit rapidity  $E_T$  to be  $E_T^{RHIC} \approx 2703$  GeV and  $E_T^{LHC} \approx 24572$  GeV respectively.

Compare these numbers to results presented recently by Kajantie [26] for the mini-jet energy (computed for  $p_t > p_{sat}$ , where  $p_{sat}$  is a saturation scale akin to  $Q_s$ ). He obtains  $E_T^{RHIC} = 2500$  GeV and  $E_T^{LHC} = 12000$ . The remarkable closeness between our results for RHIC is very likely a coincidence. Kajantie's result includes a  $K$  factor of 1.5—estimates range from 1.5–2.5 [27]. If we pick a recent value of  $K \approx 2$  [28], we obtain as our final estimate,  $E_T^{RHIC} \approx 5406$  GeV and  $E_T^{LHC} \approx 49144$  GeV.

To summarize, we performed a non-perturbative, numerical computation, for a SU(2) gauge theory, of the initial energy, per unit rapidity, of gluons produced in very high energy nuclear collisions. Extrapolating our results to SU(3), we estimated the initial energy per unit rapidity at RHIC and LHC. We plan to improve our estimates by performing our numerical analysis for SU(3). Moreover, computations in progress to determine the energy and number distributions should enable us to match our results at large transverse momenta to mini-jet calculations [24].

## Acknowledgments

We would like to thank Dr. Frank Paige and Dr. Efstratios Efstathiadis for their help in using the BNL CCD Linux cluster. R.V. acknowledges the support of DOE Nuclear Theory at BNL and A.K. acknowledges the support of the Portuguese Fundação para a Ciência e a Tecnologia, grant CERN/P/FIS/1203/98. A.K. is grateful to the BNL Physics Department for hospitality during the course of this work. R.V. would like to thank Larry McLerran and Al Mueller for useful discussions.

## References

- [1] see for instance, the proceedings of *Quark Matter 97*, *Nuc. Phys.* **A638** 329, (1998).
- [2] K. Kajantie, P. V. Landshoff, and J. Lindfors, *Phys. Rev. Lett.* **59** (1987) 2527; K. J. Eskola, K. Kajantie, and J. Lindfors, *Nucl. Phys.* **323** (1989) 37; J.-P. Blaizot and A. H. Mueller, *Nucl. Phys.* **B289** (1987) 847.
- [3] X.-N. Wang, *Phys. Rep.* **280** 287 (1997).
- [4] K. Geiger, *Phys.Rep.* **258** 237 (1995); B. Zhang, *Comput. Phys. Commun.* **104** (1997) 70.
- [5] K. J. Eskola, B. Müller, and X.-N. Wang, nucl-th/9608013; *Phys. Lett.* **374** (1996) 20.
- [6] A. H. Mueller, hep-ph/9904404.
- [7] R. Venugopalan, hep-ph/9907209.
- [8] L. McLerran and R. Venugopalan, *Phys. Rev.* **D49** 2233 (1994); **D49** 3352 (1994); **D50** 2225 (1994).
- [9] J. Jalilian-Marian, A. Kovner, L. McLerran, and H. Weigert, *Phys. Rev.* **D55** (1997) 5414.

- [10] J. Jalilian-Marian, A. Kovner, A. Leonidov, and H. Weigert, *Nucl. Phys.* **B504** 415 (1997); *Phys. Rev.* **D59** 034007 (1999); Erratum-*ibid.* **D59** 099903 (1999); J. Jalilian-Marian, A. Kovner, and H. Weigert, *Phys. Rev.* **D59** 014015 (1999); L. McLerran and R. Venugopalan, *Phys. Rev.* **D59** 094002 (1999).
- [11] M. Gyulassy and L. McLerran, *Phys. Rev.* **C56** (1997) 2219.
- [12] Yu. V. Kovchegov, *Phys. Rev.* **D54** 5463 (1996); **D55** 5445 (1997).
- [13] A. Kovner, L. McLerran and H. Weigert, *Phys. Rev* **D52** 3809 (1995); **D52** 6231 (1995).
- [14] I. Balitsky, *Phys. Rev.* **D60** 014020 (1999).
- [15] Y. V. Kovchegov and D. H. Rischke, *Phys. Rev.* **C56** (1997) 1084.
- [16] S. G. Matinyan, B. Müller and D. H. Rischke, *Phys. Rev.* **C56** (1997) 2191; *Phys. Rev.* **C57** (1998) 1927.
- [17] Xiao-feng Guo, *Phys. Rev.* **D59** 094017 (1999).
- [18] J. F. Gunion and G. Bertsch, *Phys. Rev.* **D25** (1982) 746.
- [19] A. Krasnitz and R. Venugopalan, hep-ph/9706329, hep-ph/9808332.
- [20] A. Krasnitz and R. Venugopalan, hep-ph/9809433, *Nucl. Phys.* **B**, in press.
- [21] R. V. Gavai and R. Venugopalan, *Phys. Rev.* **D54** 5795 (1996).
- [22] J. D. Bjorken, *Phys.Rev.* **D27** 140 (1983).
- [23] Y. V. Kovchegov and A. H. Mueller *Nucl. Phys.* **B529** 451 (1998).
- [24] A. Krasnitz and R. Venugopalan, in progress.
- [25] A. H. Mueller, hep-ph/9906322.
- [26] K. Kajantie, hep-ph/9907544.
- [27] K. J. Eskola and K. Kajantie, *Z. Phys.* **C75** 515 (1997).
- [28] A. Leonidov and D. Ostrovsky, hep-ph/9811417.
- [29] See Refs. [6] and Ref. [7] for a discussion. Also, if  $Q_s \sim 1$  GeV for RHIC,  $Q_s \sim \kappa \alpha_S \mu$  with  $\kappa \sim 6$ .
- [30] These considerations are also valid for non-central collisions of identical nuclei. For nuclei with unequal  $A$ , one has  $\mu_1$  and  $\mu_2$  for the two nuclei. In this case, perturbatively one expects  $\mu = \sqrt{\mu_1 \mu_2}$ .

- [31] In general,  $\varepsilon\tau$  has the physical interpretation of an energy only at asymptotic  $\tau$ . We see that it converges to a constant value at a finite  $\tau$ —and that the rate of convergence is controlled by  $\tau_D$ .
- [32] The central values of  $\gamma$  are from uncorrelated fits to the  $g^2\mu\tau$  history of  $\varepsilon\tau/(g^2\mu)^3$ . The errors on  $\gamma$  were obtained by multiplying the naive errors from the uncorrelated fit by the square root of the number of degrees of freedom. This procedure suffices for a qualitative estimate of the gluon energy density in this work. A more rigorous error analysis would require a correlated fit which cannot be reliably performed with our current relatively small data samples.

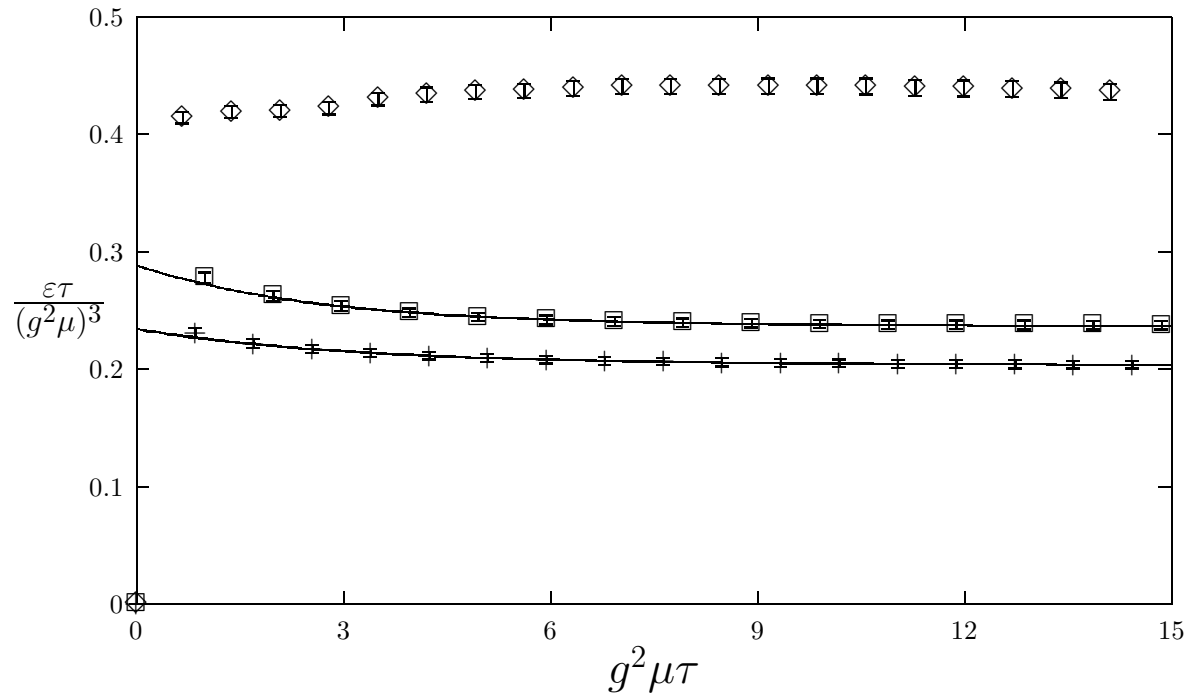


Figure 1:  $\varepsilon\tau/(g^2\mu)^3$  as a function of  $g^2\mu\tau$  for  $g^2\mu L = 5.66$  (diamonds), 35.36 (pluses) and 296.98 (squares). Both axes are in dimensionless units. Note that  $\varepsilon\tau = 0$  at  $\tau = 0$  for all  $g^2\mu L$ . The lines are exponential fits  $\alpha + \beta e^{-\gamma\tau}$  including all points beyond the peak.

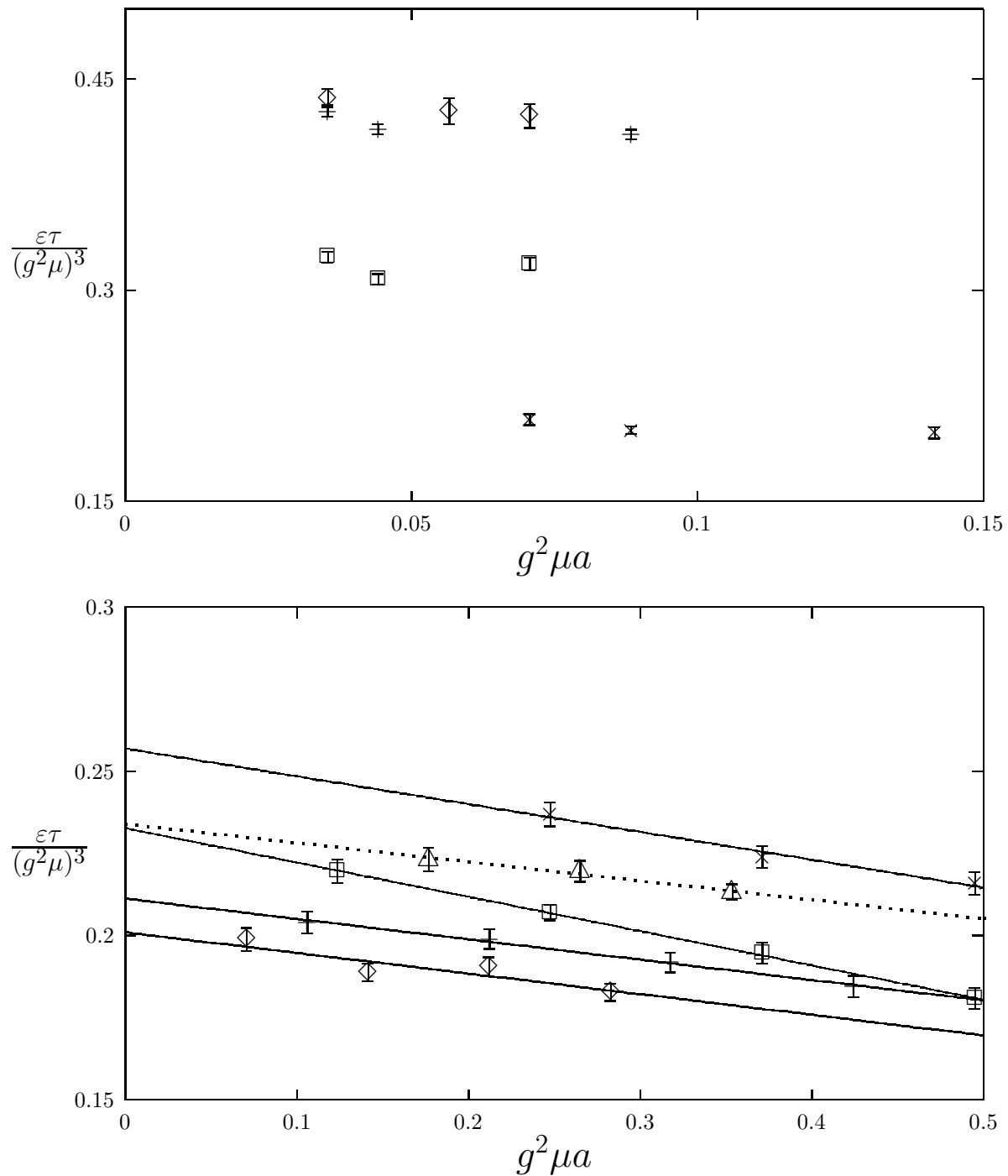


Figure 2:  $\varepsilon\tau/(g^2\mu)^3$  as a function of  $g^2\mu a$ . The points in the upper plot correspond to  $g^2\mu L = 5.66$  (diamonds), 8.84 (pluses), 17.68 (squares), and 35.36 (x's). The lower plot has  $g^2\mu L = 70.7$  (diamonds), 106.06 (pluses), 148.49 (squares), 212.13 (triangles) and 296.98 (x's). Lines in the lower plot are fits of form  $a - b \cdot x$ . The  $g^2\mu a$  ranges are different in the two halves. The points in the upper half are typically closer to the continuum limit.

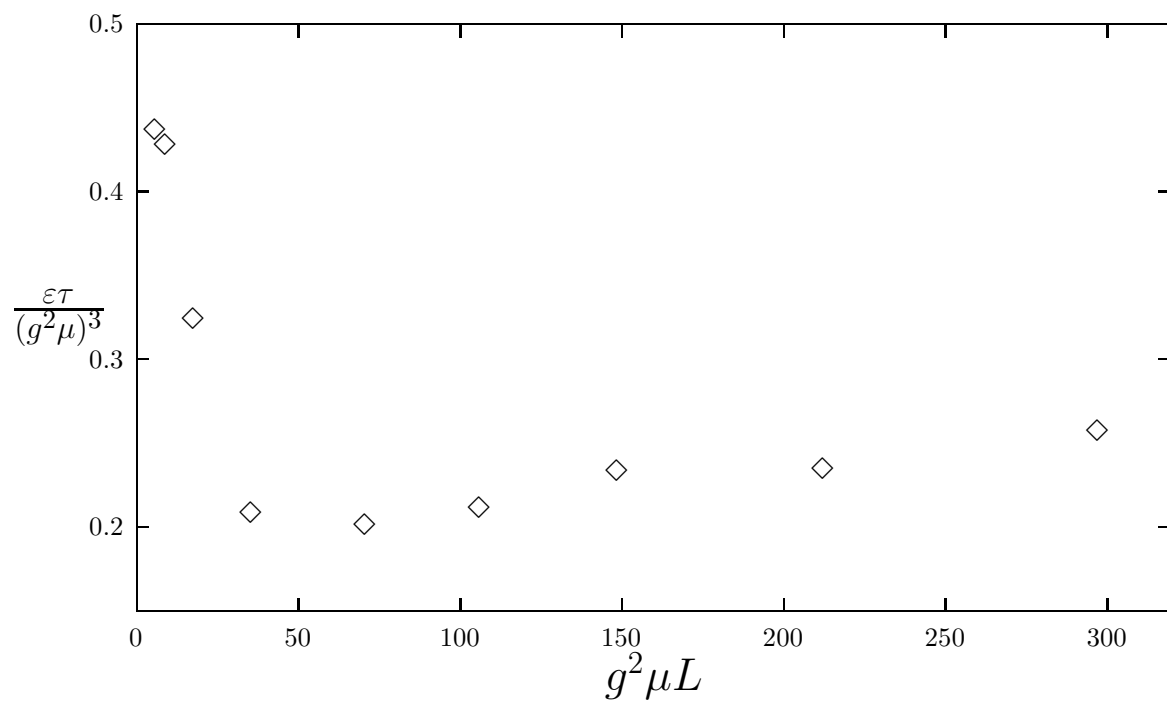


Figure 3:  $\varepsilon\tau/(g^2\mu)^3$  extrapolated to the continuum limit:  $f$  as a function of  $g^2\mu L$ . The error bars are smaller than the plotting symbols.